ECCOMAS Congress 2016
VII European Congress on Computational Methods in Applied Sciences and Engineering
M. Papadrakakis, V. Papadopoulos, G. Stefanou, V. Plevris (eds.)
Crete Island, Greece, 5–10 June 2016

APPLICATION OF SYNTHETIC JETS ACTUATORS IN WING-PYLON JUNCTION AREA TO IMPROVE THE HIGH LIFT PERFORMANCES

P. Vrchota[1]

[1] VZLU, Vyzkumny a zkusebni letecky ustav a.s., Czech Republic
address
e-mail: vrchota@vzlu.cz

Keywords: high-lift, Synthetic Jet Actuator, Computational Methods.

Abstract. *Synthetic jets actuators that produce a zero net mass flow rate have been locally applied at the pylon-wing junction to suppress the high-lift penalties caused by the closely coupled engine integration. The high fidelity numerical simulations utilizing unsteady Reynolds-averaged Navier-Stokes have been performed to simulate this problem. A wind tunnel model representing a 2,5D wing with pylon, nacelle and deployed high-lift devices is used for this study. Active flow control applied at the wing-pylon junction area can prevent the larger flow separation on the wing behind the nacelle caused by the slat cutback, increase the lift and to postpone the stall angle by interaction of the vortices from the SJA with vortices dominating this region. The performed unsteady CFD simulations demonstrate the possibility locally affect the flow by utilization of AFC. The geometrical setup of the actuators and the flow variables (blowing coefficient, actuation frequency) have been varied, as well. Two different shapes and positions of the nacelle's strike have also been considered during the simulations. The positive effect of the application of the SJA on maximum lift and stall angle has been observed.*

1 INTRODUCTION

Utilization of the Ultra-High Bypass Ration (UHBR) engine in air transport is driven by ecological and economical aspects. These new engines have lower emissions of CO2 and NOx, higher efficiency and smaller fuel consumption. On the other hand the integration of UHBR engine is very challenging part from two aspects, at least. The first one is the high-lift conditions at high angles of attack and low-speeds and the second one is connected with the clearance between the runway surface and the nacelle. To avoid longer landing gear struts suffering from weight and space penalties, the nacelle should closely-coupled to the wing. This closely-coupled integration causes the high-lift penalties due to the high-lift devices cut-back to prevent clashes with the nacelle or thrust reverser [1]. Among other techniques the Active Flow Control (AFC) can be successfully applied to remedy this lift lost due to the high-lift devices cut-back.

Within the European project AFLoNext [2] one of the main goals is the application of Active Flow Control (AFC) techniques, like pulsed jet blowing and Synthetic Jet Actuators (SJA), on wing/pylon junction to remedy the lift losses caused by in closely-coupled engine integration. A significant effort of experimental and numerical investigation of the application of the passive and AFC techniques to locally suppress the flow separation or improve the high-lift performances at the wing-pylon area, outer-wing or applied to high-lift devices has been done [3-7]. This paper summarized the results of the SJA of the high-lift configuration using the CFD simulation by means of URANS approach. The effect of the momentum coefficient $C\mu$ and actuation frequency f is discussed.

2 GEOMETRICAL SET-UP

2.1 Wind tunnel model

Model used for CFD studies is based on a wing section of a generic high-lift wing, the DLR-F15 [8], which is representative for today's transport aircraft high-lift system layout. It is equipped with a slat and a single-slotted Fowler flap. Because of the AFLoNext project this model was modified to integrate pylon and nacelle. It represents 2,5D wing with sweep angle 28deg equipped with the side plates.

2.2 Strake configurations

Two different strake's configurations were used during this study. They differ in the shape and location on the nacelle. Both strakes are depicted in Figure 1. The new strake is located closer to the wing to be more effective and creates stronger strake's vortex. The effect of the original and new strake on baseline flowfield is described in subsequent section.

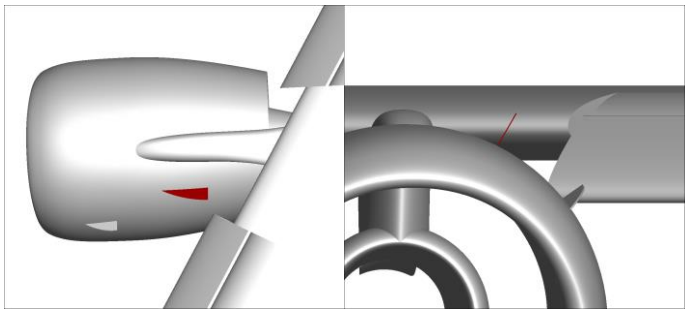

Figure 1 Position of old (grey) and new strake (red) on nacelle

2.3 Actuator's geometry and position

The circular actuator with area $5mm^2$ was used for simulation of the synthetic jet. Two configurations of the actuators were used during this study. They differ in the location and number of actuators. The first configuration is characterized by two rows of actuators located at 0.01% and 0.021% of the chord of the wing. The spanwise position of this configuration with two rows of actuators is limited by the inner slat-end on one side and the pylon's axis on the other side. The actuators in the second row are placed in cascade regarding the actuators in the first row. The second configuration was created from the first one by omitting the second row of actuator. One halve of actuators is considered in comparison with the first configuration. The spanwise location remained the same. The spanwise spacing between the actuators is 0.01m.

Actuators of both configurations were placed parallel with the leading edge and inclined 30deg towards the wing's surface. The actuators' cavities were physically modeled to enable the development of boundary layer inside them.

3 NUMERICAL METHODS

3.1 Grid creation

All grids used during this study were created in Pointwise grid generation software. The grids are unstructured with rectangular elements on the model surfaces and with tetrahedral elements in the volume. The boundary layer is simulated by prismatic elements and the condition of y+ bellow 1 was fulfilled. The region of interest was refined to capture all flow phenomena (interaction of the vortices, flow separation,…). In case that the modification of the strake or actuator's positions was considered, the same grid topology was used. Only the blocking of the surface grid on the nacelle and in the region of actuators was modified due to new strake and different actuators locations, the number of nodes remained the same. The grid in the region of interest was not changed.

3.2 Boundary conditions and CFD solver

Mass flow inlet/outlet boundary conditions (BC) were used to simulate the flow from SJA. The mass flow, total temperature and flow direction are defined at these BC. The adjusted mass flow corresponds to the required blowing velocity at the cavity's outlet. The simulation of the synthetic jet is done by switching between the mass flow inlet and mass flow outlet boundary condition controlled by harmonic (or step) function. It is possible to define the desired peak velocity and frequency of the synthetic jet using the harmonic function. In case that the step function is used, the duty cycle can be also controlled. The typical course of the mass flow in time for synthetic jet actuator is depicted in Figure 2. The cavities of the actuators were physically modeled during the mesh generation process to enable the development of boundary layer velocity profile inside them. The boundary conditions were applied at the bottom part of these cavities. The fully modeled cavities have some drawback in terms of the grid creation, number of cells etc., but the flow at the cavities' outlets is more realistic. On the other hand same effort has been devoted to applying the surface boundary conditions simulating the flow from actuators and actuation models in the past [7, 9-11].

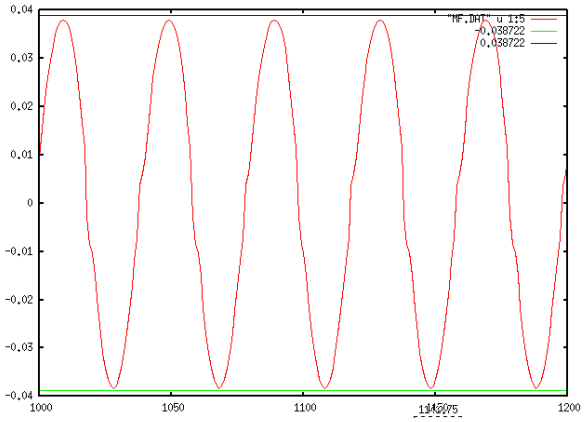

Figure 2 Typical course of the mass flow during the simulation of synthetic jet

3.3 Flow conditions

All of the computations were performed at a chord-based Reynolds number of $Re=4.65 \cdot 10^6$, the freestream Mach number 0.2 and freestream pressure corresponded to the 0m International Standard Atmosphere. These flow conditions correspond to the landing conditions of the characteristic airliner.

3.4 Baseline configuration – strake effect

The effect of the strake on the local flowfield has been experimentally and numerically investigated in the past [12]. It is usually used to remedy the lift losses due to the slat cut-back. During this study it was found that the original strake did not affect the flow as it was expected. The strake's vortex was too high above the wing and applying the AFC it transported low momentum flow towards the wing. It was the main reason to use a new strake design by DLR during the AFLoNext project. The new strake has been moved towards the wing's leading edge and it is slightly larger than the original one. The position of this strake was verified by numerical simulations performed also by DLR.

The comparison of the lift curves of the original and new strake configurations is depicted in Figure 3. It can be seen that the new strake has a significant effect on the local flowfied behind the nacelle at stall condition and it is able to improve the lift more effectively than the original one. The new strake creates stronger vortex which is closer to the wing and more interacts with the vortices dominating this region.

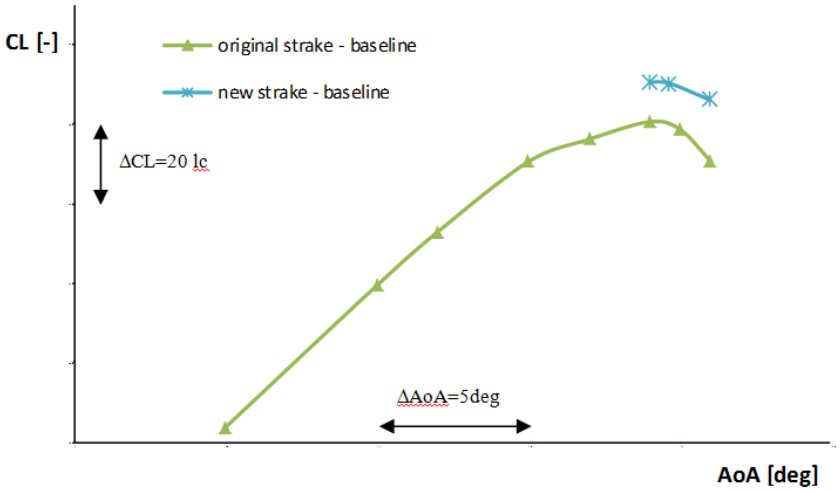

Figure 3 Effect of strakes on baseline flow

The surface streamlines together with the area of separated flow (visualized by negative x component of the skin friction coefficient) of the baseline flow with original strake are depicted in Figure 4. It is possible to see the development of the separated area with increasing AoA (depicted by the arrow). The surface streamlines and flow separation areas of the baseline flow corresponding to the configuration with the new strake is depicted in Figure 5. It is possible to see that for the same AoAs, the flow separation area is smaller in comparison with the configuration with original strake. No flow separation has been observed in the outer part of the wing (behind the pylon's axis in spanwise direction) for the simulated AoAs.

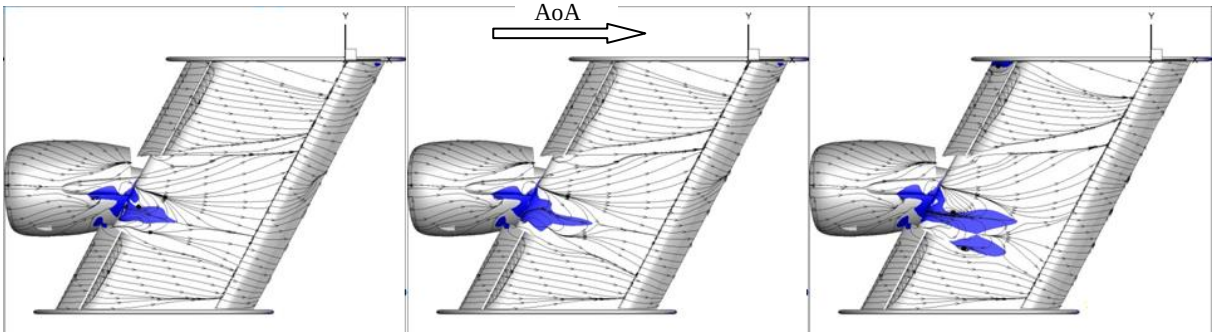

Figure 4 Surface streamlines and flow separation area (visualized by negative Cfx in blue) for baseline configuration – original strake

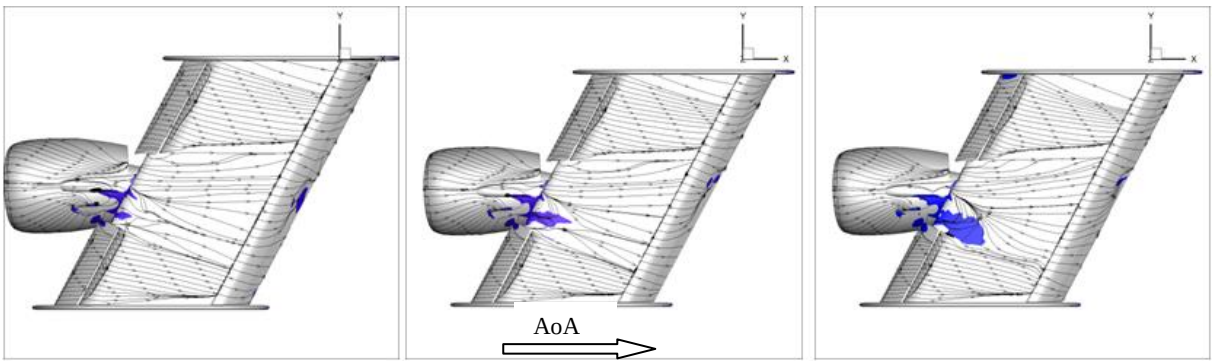

Figure 5 Surface streamlines and flow separation area for baseline configuration with new strake

The location of the flow separated area between the inner slat-end and pylon's axis was the main reason for creation of the configuration of the circular actuators with limited span wise position between the inner slat-end and pylon's axis. The configuration with the new strake was used during the CFD simulations of the SJA.

3.5 Synthetic Jet simulations

The boundary condition described in 3.2 was used for simulating of the Synthetic Jet (SJ) by means of URANS approach. A harmonic function with defined frequency and amplitude, representing the desired mass flow, was used for SJA. The frequency was limited by the limit of 100 Hz at first. A more realistic actuation frequency 1kHz has been simulated consequently. Due to extremely high time consuming simulation of the higher actuation frequency, only one post stall AoA was simulated for the configuration of the actuators in one row. The adjusted mass flow corresponded to the peak velocity 150m/s.

The configurations with one and two rows of actuators have been used to evaluate the effect of Cμ on aerodynamic performances. The frequency effect was evaluated on the configuration with one row of actuators using different actuation frequency.

From lift curves depicted in Figure 6 it is possible to see the effect of SJA with actuation frequency 100Hz (red curve) and the effect of different Cμ and f, as well. The stall angle was delayed by about 2deg in comparison with the baseline configuration. The C_{LMAX} was improved by about 8 lc according to the baseline C_{LMAX} and by about 14 lc at the same post stall AoA of the baseline configuration.

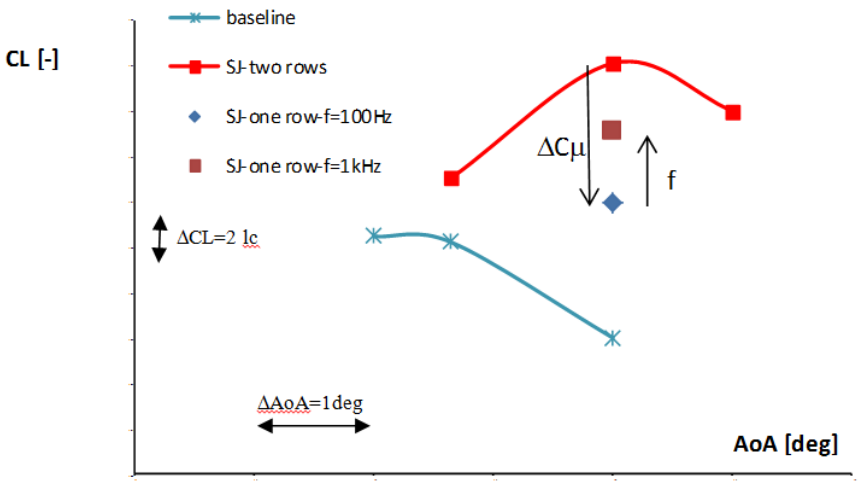

Figure 6 Lift curves and CL values of bsl and SJA of both configurations of actuators

The surface streamlines and separated areas of the configuration of two rows of SJA working with frequency 100Hz at simulated AoAs are depicted in Figure 7. It is possible to see that the separated area at stall angle is almost the same as at lower AoA due to the interaction of the synthetic jet with the inboard LE-step and slat-end vortices (see Figure 8). With increasing AoA the SJA is not able to effectively control the vortices and inboard LE-step vortex bursts and it causes the large flow separation area (see Figure 7 and Figure 8, right). The vortices for simulated AoAs are depicted in Figure 8. It is possible to see the interaction of the flow from SJA with the inboard LE-step and slat-end vortices and the discontinuity of the slat-end vortex and slightly reduced inboard LE-step vortex at post stall AoA. These vortices cannot af-

fect the flow in close vicinity of the wing and the flow separates. It has to be emphasized that these surface streamlines and vortices correspond to the last iteration of the simulations.

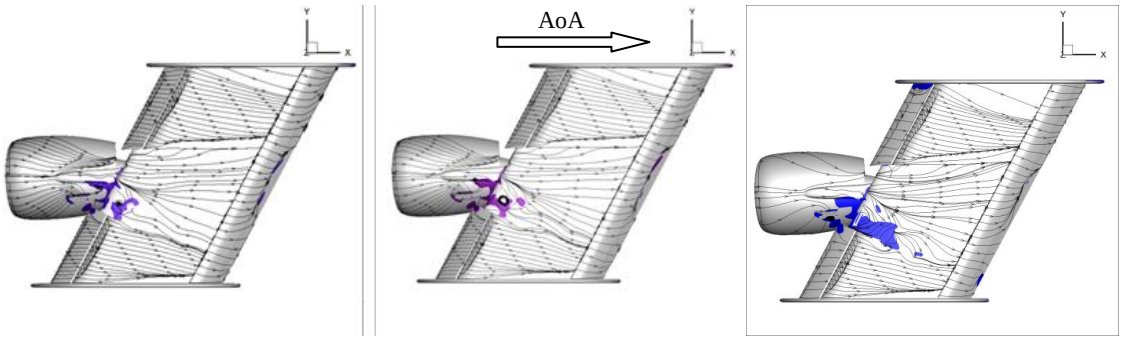

Figure 7 - Surface streamlines and flow separation area for two rows of SJA

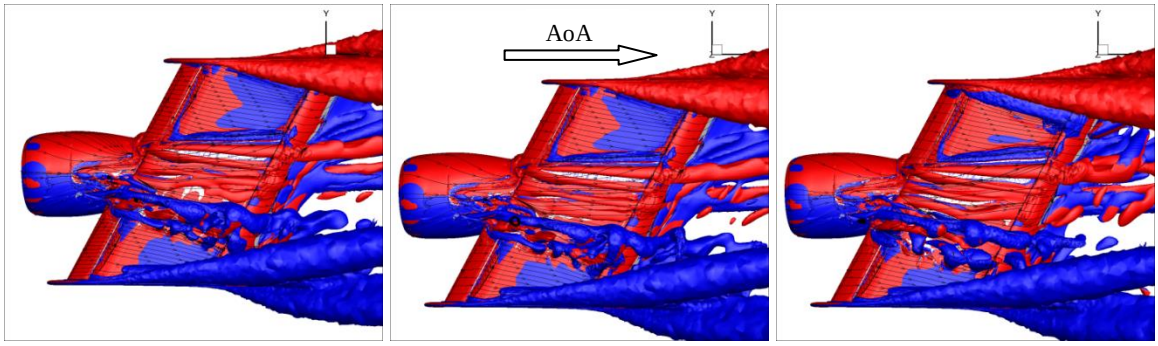

Figure 8 Vortex structures for two rows of SJA, pre-stall AoA (left), stall AoA (middle) and post stall AoA (right)

The effects of Cμ and actuation frequency on C_L at stall AoA are also depicted in Figure 6. The Cμ is decreased from 0.0252% to 0.0127% by using one row of actuators instead of two rows. The effect of reduced Cμ on the C_L is depicted in Figure 6 by the left arrow. The value of C_L is decreased by about 6 lc. The vortex structures for both values of Cμ are depicted in Figure 9 (left and middle figures). It is possible to see the positive effect of higher Cμ on the structure of the inboard LE-step and slat-end vortices. These vortices are more continuous in comparison with the vortices corresponding to the lower Cμ (one row of actuators). For the smaller Cμ the slat-end vortex is more discontinuous and the inboard LE-step vortex is slightly weaker and not so much affects the local flow close to the wing's surface.

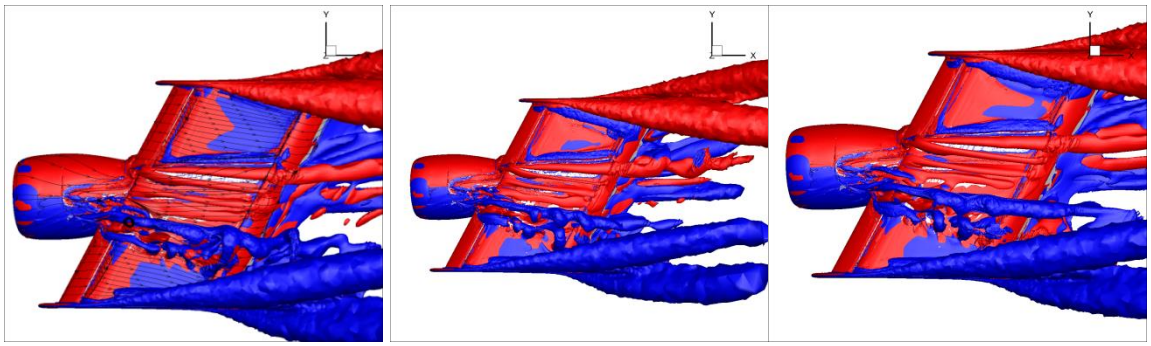

Figure 9 Effects of Cμ and actuation frequency on vortex structures, two rows of actuators (left), one row (middle) and one row of actuators with f=1000Hz (right)

In case that the one row of actuators is used (smaller Cμ) and the actuation frequency is increased from 100Hz to 1000Hz, the CL is increased by about 3 lc (see Figure 6). The right black arrow indicates the change of C_L with the change of actuation frequency. The dimensionless frequencies F^+ corresponding to the 100Hz and 1000Hz are increased from 4.79 to 47.9, respectively. The effect of actuation frequency on forming the vortex structure is depicted in Figure 9 (middle and right figures). In comparison with the lower Cμ and lower frequency (vortices in the middle), the slat-end and also the strake's vortex are more affected by SJA with higher actuation frequency. Especially the LE-step vortex is stronger.
Comparison of the flow separation areas for particular cases with SJA are depicted in Figure 10. It is possible to see that the flow separation area is increased by using smaller Cμ and on the contrary the higher actuation frequency slightly reduce it.

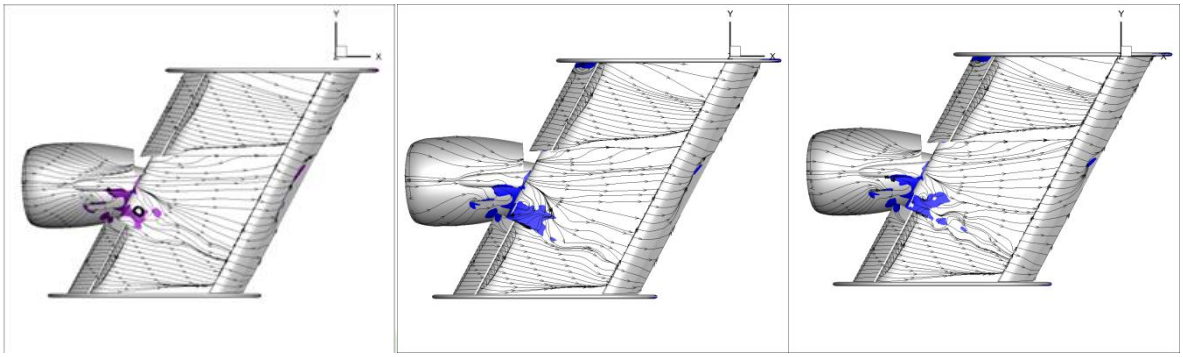

Figure 10 Surface streamlines and flow separation area of two rows of actuator (left), one row of actuator (middle) and one row of actuator with actuation frequency 1000Hz (right)

4 CONCLUSIONS

No flow separation was observed in the outboard part of the wing for the baseline and controlled flows for both strakes configurations. It was the main reason for the location of the actuators between the inner slat-end and pylon's axis.

The strake's shape and its position have a significant effect on the C_L and local flowfield without AFC. The new strake increases the C_{LMAX} by about 9 lc in comparison with the original one.

The stability and vertical position of the vortices forming behind the slat-end and inboard LE-step vortex have a significant effect on local flow separation on the wing-pylon area. If these vortices are "continuous" (not bursting or discontinuous) and closer to the wing's surface, the flow separation is usually suppressed. The structures and positions of these vortices can be, to a certain degree, maintained by a local application of AFC like SJA.

The effect of Cμ and the actuation frequency of SJA was considered and evaluated on the configuration with the new strake. The C_{LMAX} can be increased by about 8 lc by means of applying of two rows of SJ actuators with actuation frequency 100Hz. The Cμ has been changed from 0.0252% to 0.0127% by considering two rows or one row of actuators, respectively. In case that the Cμ is reduced to one half, the C_L is decreased by about 6 lc. But utilizing higher actuation frequency, the C_L can be increased again by about 3 lc. The overall drop of C_L by means of smaller value of Cμ and higher actuation frequency is only 3 lc in comparison with the value of C_L obtained using SJA in two rows and actuation frequency 100Hz.

Due to the very high time consuming of the simulations of the SJA especially with the higher actuation frequency (1000Hz), the effect of the Cμ and f was evaluated only for one post stall AoA.

The simulated high actuation frequency 1000Hz is still approximately one half of the working frequency of the real SJA. The simulation of the working frequency of SJ should be done using large eddy simulation (LES) instead of URANS, but for our target large Reynolds number it is not feasible today.

ACKNOWLEDGEMENT

These activities were done under FP7-AAT-2013-RTD-1 in the frame of AFLoNext, which is gratefully acknowledged.

Access to computing and storage facilities owned by parties and projects contributing to the National Grid Infrastructure MetaCentrum, provided under the programme "Projects of Large Infrastructure for Research, Development, and Innovations" (LM2010005), is greatly appreciated.

This work was supported by The Ministry of Education, Youth and Sports from the Large Infrastructures for Research, Experimental Development and Innovations project „IT4Innovations National Supercomputing Center – LM2015070“.

REFERENCES

[1] M. Lengers, Industrial Assessment of Overall Aircraft Driven Local Active Flow Control, *29th Congress of the International Council of the Aeronautical Sciences*, St. Petersburg, Russia, September 7-12, 2014

[2] AFLoNext project website: aflonext.eu

[3] V. Ciobaca, T. Kühn und R. Rudnik, „Active Flow Separation Control on a High-Lift Wing-Body Configuration. Part 2: The Pulsed Blowing Application,“ *29th AIAA Applied Aerodynamics Conference*, Honolulu, Hawaii, 2011.

[4] V. Ciobaca, J. Wild: Active Flow Control for an Outer Wing Model of a Take-off Transport Aircraft Configuration - A Numerical Study, *AIAA Paper 2014-2403*

[5] S. Fricke, V. Ciobaca, J. Wild, D. Norman: Numerical Studies of Active Flow Control Applied at the Engine-Wing Junction, *Advances in Simulation of Wing and Nacelle Stall Volume 131 of the series Notes on Numerical Fluid Mechanics and Multidisciplinary Design* pp 397-411

[6] M. Meunier und J. Dandois, „Simulations of Novel High-Lift Configurations Equipped with Passive and Active Means of Separation Control,“ *4th Flow Control Conference*, Seatle, Washington State, 2008-4080.

[7] P. Vrchota, P. Hospodář: Response Surface Method Application to High-Lift Configuration with Active Flow Control, Journal of Aircraft, Vol. 49, No. 6, pp. 1796-1802, 2012

[8] J. Wild, Experimental investigation of Mach- and Reynolds-number dependencies of the stall behavior of 2-element and 3-element high-lift wing sections. *AIAA-Paper 2012-0108*, 50th AIAA Aerospace Science Meeting, Nashville, 9-12 Jan. 2012.

[9] M.C. Galbraith, Numerical Simulation of a High-Lift Airfoil Employing Active Flow Control, *AIAA Paper 2006-147*

[10] R. Chow, K. Chu, G. Carpenter, Navier-Stokes Simulations of the Flow Field Around a Blown-Flap High-Lift System, *AGARD CP 515*, Sept.1993

[11] L.D. Kral, J.F. Donovan, A.B. Cain, A.W. Cary, Numerical Simulation of Synthetic Jet Actuators, AIAA Paper 1997-1834

[12] H. Frhr. v. Geyr, N. Schade: Prediction of Maximum Lift Effects on Realistic High-Lift-Commercial-Arcraft-Configurations within the European project EUROLIFT II, *Second symposium "Simulation of Wing Nacelle Stall"*, June 22-23, 2010, Braunschweig, Germany